04

The charge carriers mobility in single crystal and nanoceramics of ionic conductor $Sr_{1-x}Y_xF_{2+x}$ ($x = 0.3$)

© N.I. Sorokin

Shubnikov Institute of Crystallography of FSRC „Crystallography and Photonics" RAS, Moscow, Russia

E-mail: nsorokin1@yandex.ru

Received April 27, 2023
Revised April 27, 2023
Accepted May 4, 2023

The heterovalent solid solution $Sr_{1-x}Y_xF_{2+x}$ with fluorite structure (sp. gr. $Fm\bar{3}m$) can be synthesized in single-crystal and nanoceramic forms. Comparison of their electrical properties shows that nanoceramics have a higher ionic conductivity than single crystals the same composition. In the single-crystal state of the solid solution, the migration mechanism dominates interstitial ions F_i' in the bulk of the sample, in the nanoceramic state ther is the vacancy migration mechanism $V_F^{\bullet}$ along the grain boundaries of the sample. Using electrophysical and structural data, we calculated mobility μ_{mob} and concentration n_{mob} of ionic charge carriers in a single crystal ($a = 0.5722$ nm) and ceramics ($a = 0.57442$ nm) of composition $Sr_{0.7}Y_{0.3}F_{2.3}$. The defect mobility F_i' ($\mu_{mob} = 4.5 \cdot 10^{-10}$ cm^2/(V · s) at 500 K) in a single crystal is less than the mobility of vacancies $V_F^{\bullet}$ in nanoceramics by 140 times. The concentration charge carriers is $n_{mob} = 1.1 \cdot 10^{21}$ and $6.9 \cdot 10^{21}$ cm^{-3} (2.2 and 14.2% of the total number of anions) for single crystal and nanoceramics, respectively.

Keywords: ionic conductivity, fluorides, crystal growth, ceramic synthesis, fluorite structure, defects.

DOI: 10.21883/PSS.2023.06.56113.71

1. Introduction

SrF_2 with fluorite structure — space group (sp. gr.) $Fm\bar{3}m$ is the initial matrix for the synthesis of large amount of heterovalent solid solutions or nonstoichiometric phases $Sr_{1-x}R_xF_{2+(m-2)x}$ ($m = 3$, 4), having unipolar anionic conductivity, in condensed SrF_2-RF_3 (R = La–Lu, Y, Sc, Bi, In) and SrF_2-RF_4 (R = Th, U) systems [1–8]. They include $Sr_{1-x}Y_xF_{2+x}$ (x solid solution — mole fraction YF_3). Injection of YF_3 in SrF_2 matrix results in formation of $Sr_{1-x}Y_xF_{2+x}$ fluorite solid solution with variable number of atoms in the lattice cell and limit concentration 41 mol.% YF_3 ($x = 0.41$) in SrF_2-YF_3 [9,10] system at an eutectic temperature of 1118°C. With temperature reduction, the fluorite phase homogeneity region becomes very narrow achieving 25 mol.% YF_3 at 900°C.

Ionic conductivity $\sigma_{dc}(T)$ of nonstoichiometric $Sr_{1-x}Y_xF_{2+x}$ fluorites was initially investigated on polycrystalline samples (microceramics) [6] and single-crystals [1–4]. Investigations of single-crystals from the family of isostructural ionic conductors $Sr_{1-x}R_xF_{2+x}$ (R — rare earth elements) [1–4] have detected that solid solution with $R = Y$ has low σ_{dc}. Thus, σ_{dc} at 500 K for $Sr_{0.8}Y_{0.2}F_{2.2}$ crystal is $\sim 4 \cdot 10^3$ times lower than that of $Sr_{0.8}La_{0.2}F_{2.2}$ [2].

$Sr_{1-x}Y_xF_{2+x}$ solid solution illustrates nontypical influence of the heterovalent isomorphism on the ion conductive properties of fluorite nonstoichiometric fluorides. Compared with $Pb_{1-x}Y_xF_{2+x}$ solid solution [11–14] being the nearest structural equivalnet of $Sr_{1-x}Y_xF_{2+x}$, even higher concentrations of YF_3 impurity component in SrF_2 matrix do not bring the anionic sublattice into the superionic state. The value of $\sigma_{dc}(x)$ of concentrated $Sr_{1-x}Y_xF_{2+x}$ solid solutions with $x = 0.2$ remains at the electrical conductivity level of low-doped matrix $SrF_2:Y^{3+}$ ($x = 0.001-0.01$) [2,4,15,16].

In [6], maximum at $x = 0.15$ was observed on the concentration dependence of conductivity $\sigma_{dc}(x)$ of $Sr_{1-x}Y_xF_{2+x}$ ($0 \le x \le 0.3$) polycrystals. However, no electrical conductivity maximum was found on $\sigma_{dc}(x)$ for $Sr_{1-x}Y_xF_{2+x}$ ($0.05 \le x \le 0.2$) single-crystals [4], and a small growth of σ_{dc} was observed in the studied range of compositions.

The conductometric investigations of $Sr_{1-x}Y_xF_{2+x}$ solid solution were further continued in the concentration region $0 \le x \le 0.5$ using nanoceramic samples produced by mechanochemical synthesis and sol-gel method [17,18]. In [18], thorough measurements of frequency vs. electrical conductivity dependences $\sigma_{ac}(\nu)$ were carried out for $Sr_{0.7}Y_{0.3}F_{2.3}$ nanoceramics. This experimental data allow to calculate the mobility of charge carriers in a nanoceramic sample using the Almond–West formalism [19]. Previously in [20], this method was used to determine and compare mobility μ_{mob} and concentration n_{mob} of charge carriers in the single-crystal and nanoceramics of fluorite isovalent $Pb_{1-x}Sn_xF_2$ ($x = 0.2$) solid solution.

The objective of this study is to perform comparative analysis of microscopic properties of the ion transport in the single-crystal and nanoceramics of heterovalent $Sr_{1-x}Y_xF_{2+x}$ solid solution with the fluorite structure.

2. Summary of synthesis methods and ionic conductivity measurements in $Sr_{1-x}Y_xF_{2+x}$ single-crystals and nanoceramics

Nonstoichiometric $Sr_{1-x}Y_xF_{2+x}$ fluorite may be synthesized in different process forms: as microceramics (solid-phase method), single-crystals (directional solidification from melt) and nanoceramics (mechanochemical and sol-gel methods). $Sr_{1-x}Y_xF_{2+x}$ $(0 \le x \le 0.3)$ microceramics [6] was prepared by solid-state reaction of SrF_2 and YF_3 components placed in sealed gold tubes at 1000°C during 15 h in N_2 atmosphere. The solid solution lattice constant varies from 0.5800 $(x = 0)$ to 0.5700 ± 0.0005 nm $(x = 0.3)$.

$Sr_{1-x}Y_xF_{2+x}$ $(0.05 \le x \le 0.2)$ single-crystals [1–4] were grown from melt using the Bridgman directional solidification method. To suppress the pyrohydrolysis reaction typical for fluorides, experiments were carried out in fluorinating atmosphere (CF_4 or PTFE pyrolysis products). Crystal growth is complicated by a large difference between melting points of SrF_2 $(1464 \pm 5°C)$ and YF_3 $(1152 \pm 10°C)$.

$Sr_{1-x}Y_xF_{2+x}$ nanopowders were prepared by mechanochemical synthesis with a grinding rate of 600 rpm during 10 h (average grain size $B_{gr} = 7-16$ nm [17] and 10–36 nm [18], atmosphere is not specified) and sol-gel method ($B_{gr} = 10-45$ nm [17]). Non-equilibrium $Sr_{1-x}Y_xF_{2+x}$ fluorite powders contaned up to 50 mol.% YF_3, which is higher than the upper homogeneity region boundary (41 mol.% YF_3) of the equilibrium solid solution in SrF_2-YF_3 system [9,10]. The solid solution lattice constant varies from 0.58040 $(x = 0)$ to 0.57442 nm $(x = 0.3)$. For electrophysical investigations, ceramic pellets 8 mm in diameter and 0.5–1 mm in thickness were pressed from nanofluoride powders.

Figure 1 shows concentration dependences of the lattice cell constant for equilibrium and non-equilibrium compositions of $Sr_{1-x}Y_xF_{2+x}$ solid solutions. With $x = 0.3$, deviation of the lattice constant of non-equilibrium composition from that of the equilibrium compositions is ± 0.0022 nm.

Concentration dependences of conductivity $\sigma_{dc}(x)$ at 500 K for single-crystals, nanoceramics and microceramics of $Sr_{1-x}Y_xF_{2+x}$ solid solution are shown in Figure 2. It can be seen that the nanoceramic form of the ionic conductor has the maximum conductivity. For this form, growth of conductivity σ_{dc} by a factor of $\sim 2 \cdot 10^3$ (with respect to SrF_2) is observed when concentration YF_3 is increasing up to 30 mol.%. σ_{dc} of $Sr_{0.7}Y_{0.3}F_{2.3}$ nanoceramics at 500 K is equal to $7.1 \cdot 10^{-5}$ S/cm. $\sigma_{dc}(x)$ of single-crystals are much lower. When YF_3 $x > 0.1$ is high, curve $\sigma_{dc}(x)$ attains its saturation. Microceramics within $0 \le x \le 0.15$ shows intermediate electrophysical properties between single-crystals and nanoceramics. With $0.15 \le x \le 0.3$, electrical conductivity of microceramics becomes lower than that of single-crystals due to high resistance of grain boundaries.

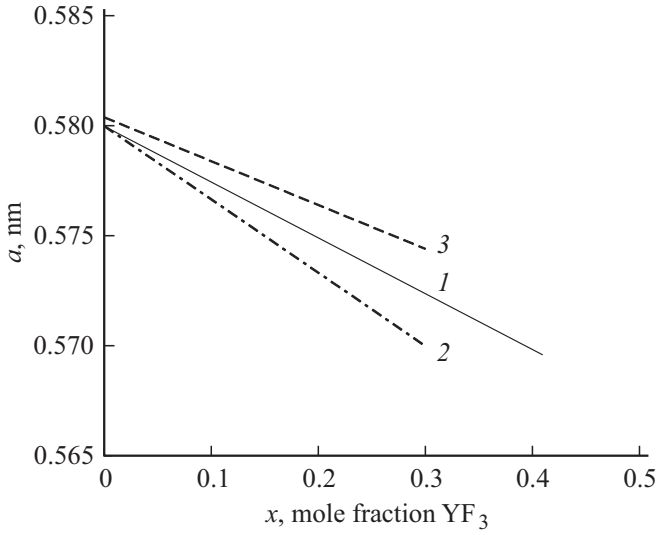

Figure 1. Concentration dependence of lattice cell constant $a(x)$ of heterovalent $Sr_{1-x}Y_xF_{2+x}$ solid solution: *1* — equilibrium state, solid-phase synthesis [21]; *2* — non-equilibrium state, solid-phase synthesis [6]; *3* — non-equilibrium state, mechanochemical synthesis [18].

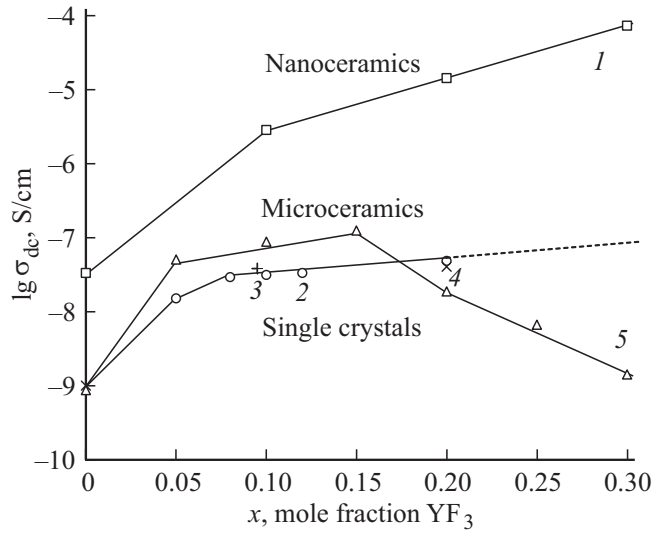

Figure 2. Concentration dependence of ionic conductivity $\sigma_{dc}(x)$ at 500 K for heterovalent $Sr_{1-x}Y_xF_{2+x}$ $(0 < x \le 0.3)$ solid solution: *1* — nanoceramics [18], *2* — single-crystals [4], *3* — single-crystals [1], *4* — single-crystals [2], *5* — polycrystals [6].

For comparison, the table shows ionic conductivity of $Sr_{1-x}Y_xF_{2+x}$ samples synthesized in different process forms. Ionic conductivity at 500 K $\sigma_{dc} = 1.4 \cdot 10^{-5}$ S/cm [18] of $Sr_{0.8}Y_{0.2}F_{2.2}$ nanoceramics exceeds the electrical conductivity of a single-crystal with the same composition ($4.0 \cdot 10^{-8}$ S/cm [2], $4.8 \cdot 10^{-8}$ S/cm [4]) by a factor of 300–350. Extrapolated ionic conductivity of $Sr_{0.7}Y_{0.3}F_{2.3}$ single-crystal required for further calculations is equal to $8 \cdot 10^{-8}$ S/cm.

The Frenkel–Arrhenius equation parameters $\sigma_{dc}\ T = \sigma_0 \exp(-H_\sigma/k_B T)$ for ionic conductivity of $Sr_{1-x}Y_xF_{2+x}$ solid solution in nanoceramic and single-crystalline form

Composition x of $Sr_{1-x}Y_xF_{2+x}$ solid solution	Form of material	Multiplier σ_0, 10^5 SK/cm	Enthalpy H_σ, eV	Literature
0	Nanoceramics	0.12	0.88	[18]
0.1		2.0	0.81	
0.2		2.0	0.74	
0.3		2.0	0.67	
0*	Single-crystals	98	1.317	[2]
0.05		3.7	1.06	[4]
0.08		5.5	1.05	
0.095		7.2	1.05	[1]
0.1		7.4	1.06	[4]
0.12		8.0	1.06	
0.15		1.2	1.10	
0.2		5.7 3.5	1.03 1.016	[4] [2]

Note * The crytal contained 0.2 mol.% LaF_3.

3. Calculation of charge carrier mobility in $Sr_{0.7}Y_{0.3}F_{2.3}$ single-crystal within a crystal-physical model

Heterovalent substitutions of Sr^{2+} by R^{3+} result in occurrence of fluorine ions F_i' in interstitial positions and fluorine vacancies $V_F^\bullet$ in $Sr_{1-x}R_xF_{2+x}$ (R = La–Lu, Y) solid solution structures to overcome short interionic distances $F^- - F^-$. Strong Coulomb interactions between large concentrations of „crystal-chemical" anion and cation point defects induce non-mobile defect associates (structural clusters) [22–24]. In $Sr_{1-x}R_xF_{2+x}$ single-crystals, hopping ion transport mechanism takes place which is associated with migration of mobile interstitial fluorine ions F_i' over structural positions of anion sublattice [2–4,6,8].

According to X-ray diffraction examinations [25,26], underpopulation of main fluorine positions 8c sp. gr. $Fm\bar{3}m$ (vacancies $V_F^\bullet$) and population of interstitial positions 48i (interstitial ions F_i'(48i)) are observed near interstitial position 4b in $Sr_{1-x}Y_xF_{2+x}$ fluorite crystal with $x = 0.1$. Point defects $V_F^\bullet$ (in eight cube corners) and F_i'(48i) (in twelve cubooctahedron corners) form structural clusters $[Sr_8Y_6F_{69}]$. Cluster $[Sr_8Y_6F_{69}]$ also contains interstitial F_i'(4b) in position 4b in the center of this cluster.

Cluster $[Sr_8Y_6F_{69}]^{35-}$ is charged with respect to the structural fragment of $[Sr_{14}F_{64}]^{36-}$ fluorite lattice. Heterovalent substitution pattern in $Sr_{1-x}Y_xF_{2+x}$ crystals is written as [24]

$$[Sr_{14}F_{64}]^{\times}_{Sr14F64} \rightarrow [Sr_8Y_6F_{69}]^{\bullet}_{Sr14F64} + F'_{mob}, \qquad (1)$$

where F'_{mob} is the interstitial fluorine ion in position 4b outside the cluster. As a result, two interstitial defects F_i'(4b) fall on one $[Sr_8Y_6F_{69}]$ cluster: one of them is in the cluster center and the other is outside the cluster.

Per one $[Sr_8Y_6F_{69}]$ cluster, the number of interstitial ions in positions 4b is 6 times as low as their number in positions 48i. Therefore, population of interstitial position 4b near position 48i usually was not clarified in the X-ray diffraction analysis: e. g., in structural investigations of $Sr_{1-x}Y_xF_{2+x}$ [25,26] and $Ca_{1-x}Y_xF_{2+x}$ [27] crystaks at $x = 0.1$. Interstitial fluorines F'_{mob} not included in the clusters and located near the clusters are charge carriers [24]. In thermal activation conditions, they are involved in the hopping ion transition mechanism in $Sr_{1-x}Y_xF_{2+x}$ fluorite crystals. Concentration of „crystal-chemical" charge carriers n_{mob} is a temperature-independent variable determined by the structural mechanism of substitution of Sr^{2+} by Y^{3+}.

Theoretical calculations [28,29] show that in anion-excessive $M_{1-x}R_xF_{2+x}$ (M = Ca, Sr, Ba) crystals with fluorite structure, mobile fluorine ion hops in noncollinear interstitial mechanism are most probable. fluorine ion F'_{mob} in interstitial position 4b sp. gr. $Fm\bar{3}m$ displaces the nearest anion located in main position 8c into neighboring vacant interstitial position 4b (two fluorine ions are involved in the ion transport elementary event).

Ionic conductivity of $Sr_{1-x}Y_xF_{2+x}$ crystals is determined by the product of concentration n_{mob} and mobility μ_{mob} of charge carriers

$$\sigma_{dc} = qn_{mob}\mu_{mob} = (qn_{mob}\mu_0/T)\exp[-H_h/kT], \quad (2)$$

where q is the elementary charge, μ_0 is the pre-exponential mobility factor, H_h is the activation enthalpy of anionic charge carrier hops.

For $Ba_{1-x}Y_xF_{2+x}$ solid solution, ion transport is simplified due to the large volume of the lattice cell [3]. For $Sr_{1-x}Y_xF_{2+x}$ and $Ca_{1-x}Y_xF_{2+x}$ solid solutions, ion transport is hindered, because defects F'_{mob} are closely related to the clusters resulting in high potential barriers ($H_h \approx 1$ eV) for their migration. As a result, despite the structurally disordered state of the anion sublattice, conductivity of $Sr_{1-x}Y_xF_{2+x}$ crystals is low.

In accordance with the heterovalent substitution pattern (1), one charge carrier F'_{mob} falls per one $[Sr_8Y_6F_{69}]$ cluster, therefore their concentration in $Sr_{0.7}Y_{0.3}F_{2.3}$ single-crystal is equal to

$$n_{mob} = Zx/ya^3 = 1.1 \cdot 10^{21}\,cm^{-3}, \quad (3)$$

where lattice constant $a = 0.5722$ nm [21], number of formula units in the lattice cell $Z = 4$, composition $x = 0.3$ and number of rare-earth ions in cluster $y = 6$. Concentration n_{mob} is 2.2% of the total number of anions in $Sr_{0.7}Y_{0.3}F_{2.3}$ crystal and is $1.4 \cdot 10^6$ times as high as the concentration of anti-Frenkel defects in SrF_2 fluorite matrix ($n_{mob} = 7.6 \cdot 10^{14}\,cm^{-3}$ at 500 K [16]). This fact is the direct evidence of string structural disorder in anion subsystem of $Sr_{1-x}Y_xF_{2+x}$ crystals.

Mobility of charge carriers at 500 K is

$$\mu_{mob} = \sigma_{dc}/qn_{mob} = 4.5 \cdot 10^{-10}\,cm^2/(V \cdot s). \quad (4)$$

μ_{mob} for $Sr_{0.7}Y_{0.3}F_{2.3}$ solid solution single-crystal is lower than the mobility of interstitial fluorine ions F'_i ($\mu_i = 9.3 \cdot 10^{-9}\,cm^2/(V \cdot s)$ [15]) and fluorine vacancies $V_F^{\bullet}$ ($\mu_v = 1.1 \cdot 10^{-7}\,cm^2/(V \cdot s)$ [15]) in SrF_2 fluorite matrix single-crystal. Comparison of charge carrier mobility in $Sr_{0.7}Y_{0.3}F_{2.3}$ and $Ba_{0.69}La_{0.31}F_{2.31}$ single-crystals [30] shows that it is $1.1 \cdot 10^4$ times lower in the first solid solution.

4. Calculation of charge carrier mobility in $Sr_{0.7}Y_{0.3}F_{2.3}$ nanoceramics within the Almond–West model

In $Sr_{0.7}Y_{0.3}F_{2.3}$ nanoceramics (average grain size $B_{gr} = 13$ nm) [18], the ion transport hopping mechanism dominates and is associated with migration of vacancies $V_F^{\bullet}$ over grain boundaries of the ceramic sample. Electrical conductivity activation enthalpy ($H_h = 0.67$ eV [18]) in the nanoceramics is much lower than in the single-crystal (extrapolated value $H_h \approx 1$ eV [2,4]). $H_h = 0.67$ for $Sr_{0.7}Y_{0.3}F_2$ nanoceramics coincides well with $H_h = 0.70$ eV [15] for migration of fluorine vacancies in SrF_2 crystal.

Charge carrier hop rate ν_h may be determined depending on the dynamic conductivity [19]:

$$\sigma_{ac}(\nu) = \sigma_{dc}[1 + (\nu/\nu_h)^n]. \quad (5)$$

Ion carriers participate in electrical conductivity when $\nu < \nu_h$ and in dielectric relaxation when $\nu > \nu_h$. Charge carrier mobility μ_{mob} is defined by the Nernst–Einstein relation and depends on temperature T, frequency ν_h and length d of hops.

$$\mu_{mob} = q\nu_h d^2/6k_BT. \quad (6)$$

Charge carrier hop length in the fluorite structure for conductivity-vacancy mechanism is equal to

$$d = a/2, \quad (7)$$

where a is the lattice cell constant.

From equations (2), (6) and (7), mobility μ_{mob} and concentration n_{mob} of charge carriers may be calculated. Within such approach, we have earlier determined microscopic characteristics of ion transport in $Ba_{0.69}La_{0.31}F_{2.31}$, $Pb_{0.9}Sc_{0.1}F_{2.1}$, $Pb_{0.68}Cd_{0.32}F_2$ and $Pb_{0.8}Sn_{0.2}F_2$ [20,30–32] fluorine superionics which are isostructural to $Sr_{0.7}Y_{0.3}F_{2.3}$ crystal.

From the analysis of experimental data $\sigma_{ac}(\nu)$ for $Sr_{0.7}Y_{0.3}F_{2.3}$ solid solution nanoceramics [18], we obtain $\nu_h \approx 2 \cdot 10^7$ Hz at 500 K. Then, taking into account $d = 0.28721$ nm [18], μ_{mob} at 500 K and n_{mob} are equal to $6.4 \cdot 10^{-8}\,cm^2/(V \cdot s)$ and $6.9 \cdot 10^{21}\,cm^{-3}$, respectively. Concentration of n_{mob} carriers for the nanoceramics is 14.2% of the total number of anions of $Sr_{0.7}Y_{0.3}F_{2.3}$ solid solution. Comparison of ion-conductive properties of $Sr_{0.7}Y_{0.3}F_{2.3}$ ion conductor single-crystal and nanoceramics shows that mobility of anion charge carriers in the single-crystal form is ~ 140 times as low as in the nanoceramic form.

5. Conclusion

High anionic conductivity of $Sr_{1-x}Y_xF_{2+x}$ solid solution nanoceramics is associated with the presence of mobile fluorine vacancies $V_F^{\bullet}$ at the nanoscale grain boundaries ($H_h = 0.67$ eV). Ionic conductivity of $Sr_{1-x}Y_xF_{2+x}$ single-crystals is low, despite the structural disorder of the solid solution with isomorphous substitutions of Sr^{2+} by Y^{3+}. Ion transport in $Sr_{1-x}Y_xF_{2+x}$ single-crystals is defined by hopping movements of interstitial ions F'_{mob} in the fluorite structure with high potential barriers ($H_h \approx 1$ eV). Microscopic parameters of charge carriers in single-crystal ($\mu_{mob} = 4.5 \cdot 10^{-10}\,cm^2/(V \cdot s)$, $n_{mob} = 1.1 \cdot 10^{21}\,cm^{-3}$) and nanoceramic ($\mu_{mob} = 6.4 \cdot 10^{-8}\,cm^2/(V \cdot s)$, $n_{mob} = 6.9 \cdot 10^{21}\,cm^{-3}$) forms of $Sr_{1-x}Y_xF_{2+x}$ ionic conductor with $x = 0.3$ were calculated. Mobility of charge carriers in the single-crystal is ~ 140 times as low as in the nanoceramics.

Funding

The study was supported by the Ministry of Science and Higher Education under the State Assignment of the Federal Scientific Research Center „Crystallography and Photonics“ of RAS.

Conflict of interest

The author declares that he has no conflict of interest.

References

[1] N.I. Sorokin, D.N. Karimov, E.A. Sulyanova, Z.I. Zhmurova, B.P. Sobolev. Kristallografiya **708**, 2010 (2002). (in Russian).
[2] N.I. Sorokin, M.W. Breiter. Solid State Ionics **104**, *3–4*, 325 (1997).
[3] P.P. Fedorov, T.M. Turkina, B.P. Sobolev, E. Mariani, M. Svantner. Solid State Ionics **6**, *4*, 331 (1982).
[4] A.K. Ivanov-Shits, N.I. Sorokin, P.P. Fedorov, B.P. Sobolev. Solid State Ionics **31**, *4*, 253 (1989).
[5] E.F. Hairetdinov, N.F. Uvarov, Y.J. Xu, J.M. Réau. Physica Status Solidi B **203**, *1*, 17 (1997).
[6] J.M. Réau, A. Rhandour, S.F. Matar, P. Hagenmuller. J. Solid State Chem. **55**, *1*, 7 (1984).
[7] E.F. Hairetdinov, N.F. Uvarov, M. Wahbi, J.M. Réau, X.Y. Jun, P. Hagenmuller. Solid State Ionics **86–88**, *Part 1*, 113 (1996).
[8] J.A. Archer, A.V. Chadwick, J.R. Jack, B. Zeqiri. Solid State Ionics **9–10**, *Part 1*, 505 (1983).
[9] B.P. Sobolev, E.G. Ippolitov, B.M. Zhigarnovsky, L.S. Garashina. Izv. AN SSSR. Neorgan. materialy **1**, *3*, 362 (1965). (in Russian).
[10] B.P. Sobolev, K.B. Seiranian. J. Solid State Chem. **39**, *3*, 337 (1981).
[11] V.Ya. Kavun, A.B. Slobodyuk, S.V. Gnedenkov, S.L. Sinebryukhov, V.K. Goncharuk, N.F. Uvarov, V.I. Sergienko. Zhurn. strukt. khimii **899**, **48**, 2007 (2008). (in Russian).
[12] S.J. Patwe, P. Balaya, P.S. Goyal, A.K. Tyagi. Mater. Res. Bull. **36**, *9*, 1743 (2001).
[13] N.I. Sorokin, G.A. Shchavlinskaya, I.I. Buchinskaya, B.P. Sobolev. Elektrokhimiya **1031**, 1998 (2011). (in Russian).
[14] J.M. Réau, P.P. Fedorov, L. Rabardel, S.F. Matar, P. Hagenmuller. Mater. Res. Bull. **18**, *10*, 1235 (1983).
[15] W. Bollmann. Krist. Technik **15**, *2*, 197 (1980).
[16] W. Bollmann, P. Görlich, W. Hauk, H. Mothes. Physica Status Solidi A **2**, *1*, 157 (1970).
[17] B. Ritter, T. Krahl, G. Scholz, E. Kemnitz. J. Phys. Chem. **120**, *16*, 8992 (2016).
[18] S. Breuer, B. Stanje, V. Pregartner, S. Lunghammer, I. Hanzu, M. Wilkening. Crystals **8**, *3*, 122 (2018).
[19] D.P. Almond, C.C. Hunter, A.R. West. J. Mater. Sci. **19**, *10*, 3236 (1984).
[20] N.I. Sorokin. Phys. Solid State **61**, *11*, 2014 (2019).
[21] P.P. Fedorov, B.P. Sobolev. Kristallografiya **1210**, 1992 (2002). (in Russian).
[22] E.A. Sulyanova, B.P. Sobolev. Cryst. Eng. Commun. **24**, *20*, 3762 (2022).
[23] P.P. Fedorov. Butll. Soc. Cat. Cien. **12**, *2*, 349 (1991).
[24] N.I. Sorokin, A.M. Golubev, B.P. Sobolev. Kristallografiya **59**, 275 (2014). (in Russian).
[25] L.P. Otroshchenko, V.B. Aleksandrov, B.P. Sobolev, N.N. Bydanov, V.A. Sarin, L.E. Fykin. Tez. dokl. IX Vsesoyuz. konf. po fiz. khimii i elektrokhimii ion. rasplavov i tverd. elektrolitov. Sverdlovsk (1987). p. 96. (in Russian).
[26] E.A. Sulyanova, D.N. Karimov, B.P. Sobolev. Kristallografiya **569**, 2020 (2002). (in Russian).
[27] L.P. Otroshchenko, V.B. Aleksandrov, N.N. Bydanov, V.I. Simonov, B.P. Sobolev. Kristallografiya **569**, 2020 (2002). (in Russian).
[28] I.Yu. Gotlib, I.V. Murin, I.V. Piotrovskaya, E.N. Brodskaya. Neorgan. materialy **38**, *3*, 358 (2002). (in Russian).
[29] K. Mori, A. Mineshige, T. Saito, M. Sugiura, Y. Ishikawa, F. Fujisaki, K. Namba, T. Kamijama, T. Otomo, T. Abe, T. Fukunaga. ACS Appl. Energy Mater. **3**, *3*, 2873 (2020).
[30] N.I. Sorokin, D.N. Karimov. Phys. Solid State **63**, *12*, 1821 (2021).
[31] N.I. Sorokin. Phys. Solid State **57**, *7*, 1352 (2015).
[32] N.I. Sorokin. Phys. Solid State **60**, *4*, 714 (2018).

Translated by E.Ilyinskaya